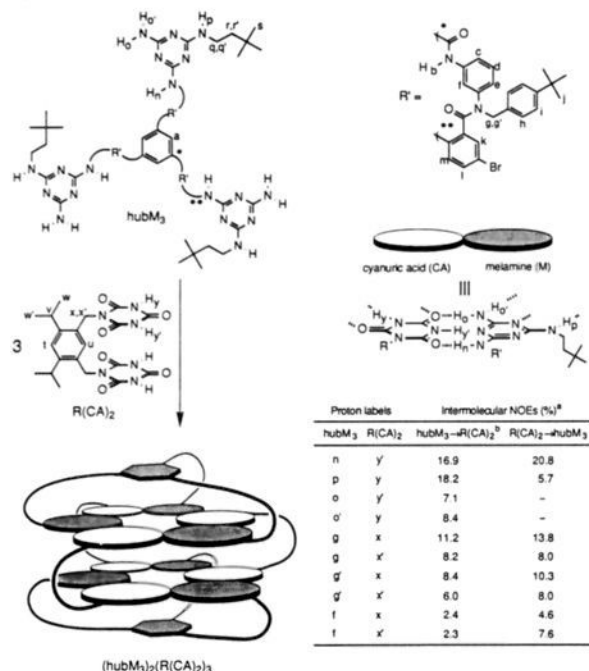


Scheme I. Self-Assembly of hubM_3 with $\text{R}(\text{CA})_2$ To Give a Supramolecular 2:3 Complex

^a Intermolecular NOEs between hubM_3 and $\text{R}(\text{CA})_2$ in the 2:3 complex are given in the table. The complex (10 mM) in CDCl_3 was degassed with five freeze-pump-thaw cycles, and the NOE difference spectra were taken at 500 MHz with a presaturation time of 3.0 s. ^b $\text{hubM}_3 \rightarrow \text{R}(\text{CA})_2$ represents irradiation of the proton on hubM_3 and observation of an NOE at the proton of $\text{R}(\text{CA})_2$.

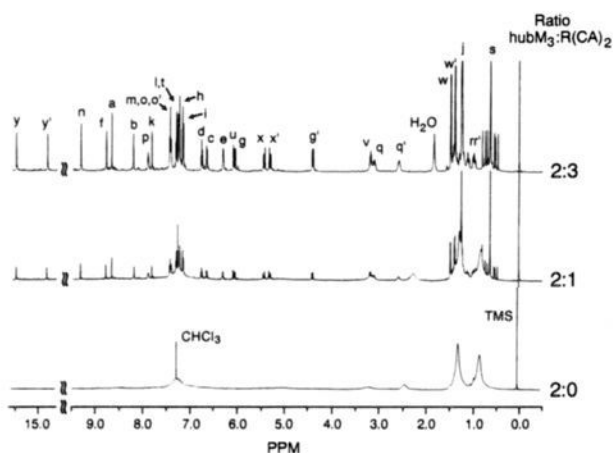


Figure 1. ^1H NMR titration of hubM_3 (500 MHz, 10 mM in CDCl_3) with $\text{R}(\text{CA})_2$. The peak assignments are shown at the top of the figure. We believe that the small peaks in the base line of the upper spectrum correspond to conformational isomers of the 2:3 complex. These minor peaks are not impurities in either of the individual components. $\text{R}(\text{CA})_2$ alone is too insoluble to give a detectable spectrum at saturation (<0.1 mM) in CDCl_3 at the instrument gain used here.

Formation of the $(\text{hubM}_3)_2(\text{R}(\text{CA})_2)_3$ complex is an unfavorable process entropically: five particles combine into a single particle; the spokes of hubM_3 are constrained to one conformation. The complex is stable only because the enthalpy gained by forming the 36 hydrogen bonds in the complex is large enough to compensate for the entropic factor.

This procedure points the way to the synthesis of large molecular assemblies by a process based on self-assembly of stable hydrogen-bonding networks, rather than formation of covalent bonds.

(6) UV data: uncomplexed hubM_3 $\lambda_{\text{max}} = 269 \text{ nm}$ ($\epsilon = 94050 \text{ M}^{-1} \text{ cm}^{-1}$); $(\text{hubM}_3)_2(\text{R}(\text{CA})_2)_3$ $\lambda_{\text{max}} = 255 \text{ nm}$ ($\epsilon = 100200 \text{ M}^{-1} \text{ cm}^{-1}$).

In that sense, its strategy is more closely modeled on the principles that determine secondary and tertiary structure in proteins and nucleic acids than on the methods used in classical organic synthesis. Future papers will describe the synthesis of structures more complex than $(\text{hubM}_3)_2(\text{R}(\text{CA})_2)_3$.

Acknowledgment. NMR instrumentation was supported by National Science Foundation Grant CHE-84-10774. We thank Professor Robert Cohen (MIT, Chemical Engineering) for the loan of the vapor pressure osmometer.

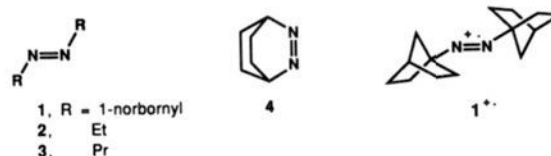
1,1'-Azonorbornane Radical Cation. A Solution-Stable Azoalkane Radical Cation

Maria E. Mendicino and Silas C. Blackstock*

Department of Chemistry, Vanderbilt University
Nashville, Tennessee 37235

Received October 5, 1990

The discovery by Engel, Shine, and co-workers¹ of fast deazetative fragmentation of 1,1'-azoadamantane upon one-electron oxidation has sparked general interest in the nature of azoalkane radical cations, their fragmentation mechanism, and their usefulness as precursors to various radical, cation, and radical cation systems.¹⁻⁶ Azoalkane radical cations are short-lived species and, to date, have been observed only under matrix-isolation conditions by low-temperature ESR spectroscopy. Some azoalkane radical cations are even too reactive to survive matrix isolation.⁴ Here we present the first example of a solution-stable azo radical cation system and report preliminary physical data for this species.



Electrochemical oxidation of 1,1'-azonorbornane⁷ (1) by cyclic voltammetry⁸ (CV) yields a chemically reversible voltammogram ($E^{\circ'} = 1.40 \text{ V}$ vs SCE, $E_{\text{pp}} = 60 \text{ mV}$), indicating a solution lifetime for $1^{+\bullet}$ of at least seconds. Chemical oxidation of 1 in cold CH_2Cl_2 by 1 molar equiv of tris(2,4-dibromophenyl)-amminium hexachloroantimonate, $\text{Ar}_3\text{N}^+\text{SbCl}_6^-$, results in decolorization of the green oxidant upon mixing. The resulting yellow solution shows a five-line ESR signal assigned as $a(2\text{N})$

(1) Bae, D. H.; Engel, P. S.; Hoque, A. K. M. M.; Keys, D. E.; Lee, W.-K.; Shaw, R. W.; Shine, H. J. *J. Am. Chem. Soc.* **1985**, *107*, 2561.

(2) (a) Engel, P. S.; Keys, D. E.; Kitamura, A. *J. Am. Chem. Soc.* **1985**, *107*, 4964. (b) Shine, H. J.; Bae, D. H.; Hoque, A. K. M. M.; Kajstura, A.; Lee, W. K.; Shaw, R. W.; Soroka, M. *Phosphorus Sulfur* **1985**, *23*, 111. (c) Engel, P. S.; Kitamura, A.; Keys, D. E. *J. Org. Chem.* **1987**, *52*, 5015.

(3) (a) Adam, W.; Casado, A.; Miranda, M. A. *Angew. Chem., Int. Ed. Engl.* **1987**, *26*, 797. (b) Adam, W.; Dorr, M. *J. Am. Chem. Soc.* **1987**, *109*, 1570. (c) Adam, W.; Grabowski, S.; Miranda, M. A.; Rubenacker, M. *J. Chem. Soc., Chem. Commun.* **1988**, 142.

(4) Blackstock, S. C.; Kochi, J. K. *J. Am. Chem. Soc.* **1987**, *109*, 2484.

(5) (a) Rhodes, C. J.; Louwries, P. W. F. *J. Chem. Res., Synop.* **1988**, 38.

(b) Rhodes, C. J. *J. Chem. Soc., Faraday Trans. 1* **1988**, *84*, 3215. (c) Rhodes, C. J. *J. Chem. Soc., Chem. Commun.* **1990**, 799.

(6) (a) Williams, F.; Guo, Q.-X.; Petillo, P. A.; Nelsen, S. F. *J. Am. Chem. Soc.* **1988**, *110*, 7887. (b) Gerson, F.; Qin, X.-Z. *Helv. Chim. Acta* **1988**, *71*, 1498.

(7) (a) Golzke, V.; Groeger, F.; Oberlinner, A.; Ruchardt, C. *Nouv. J. Chim.* **1978**, *2*, 169. (b) Schmittl, M.; Ruchardt, C. *J. Am. Chem. Soc.* **1987**, *109*, 2750. (c) Neuman, R. C., Jr.; Grow, R. H.; Binegar, G. A.; Gunderson, H. J. *J. Org. Chem.* **1990**, *55*, 2682. 1 has been prepared in 63% overall yield from 1-aminonorbornane by *m*-CPBA oxidation to 1-nitrosonorbornane followed by Si_2Cl_6 reduction of the nitroso dimer.

(8) Electrochemistry is performed at a planar Pt disk working electrode in 0.1 M TBAP/acetonitrile at room temperature at scan rates of 20–2000 mV s^{-1} .

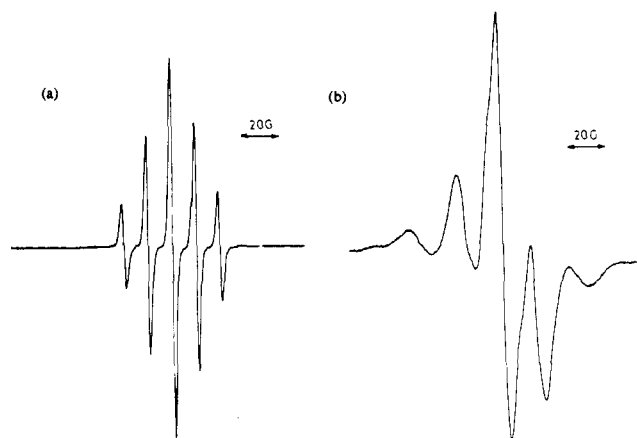


Figure 1. ESR spectra of 1,1'-azonorbornane radical cation (1^{**}), (a) from Ar_3N^+ oxidation in CH_2Cl_2 at -80°C and (b) from γ irradiation in CFCl_3 matrix at -150°C .

= 13.0 G (Figure 1a) and shows a broad optical absorption band at $\lambda_m = 370$ nm ($\epsilon = 480$). Matrix oxidation of **1** at 77 K in CFCl_3 by γ irradiation⁹ generates a yellow matrix which also displays a five-line ESR spectrum but with a splitting of 22 G (Figure 1b). Reversible transformation of the five-line ESR signal pattern in CH_2Cl_2 from 13.0 to 22.5 G upon freezing of the sample indicates that the matrix and solution-phase ESR-active species are the same.

When 1 molar equiv of thianthrene (Th, $E^\circ = 1.25$ V vs SCE) is added to the above-mentioned ESR-active yellow solution, the solution turns deep purple (the color of Th^{*+}), and upon workup with aqueous base, **1**, Ar_3N , Th, and Th *S*-oxide (ThO) are recovered quantitatively in the expected 2:2:1:1 ratio.¹⁰ This result supports our assignment of the above data to 1^{**} rather than to some other radical species derived from a secondary process that might occur subsequent to electron transfer.

We believe the 1-norbornyl substituents impart unusual kinetic stability to this azoalkane radical cation because of (a) 1-norbornyl's reluctance toward C,N bond cleavage, (b) its steric blockade of the azo functionality, and (c) its lack of reactive C,H bonds α to the azo linkage. The half-life of 1^{**} in dilute CH_2Cl_2 solution is roughly 25 min at 15°C as determined by both ESR and UV-vis signal decay rates. Thermal decomposition of 1^{**} appears to involve deazetation, since gas evolution (79% yield) accompanies the disappearance of the yellow radical cation.

A comparison of **1**'s formal oxidation potential ($E^\circ = 1.40$ V) and its vertical ionization potential ($\text{IP}_V = 8.24$ eV)¹¹ to those of a group of 41 organic molecules (consisting of fused-ring aromatics,^{12a} alkyl benzenes,^{12b} and bicyclic peroxides^{12c}) whose one-electron oxidation is accompanied by little geometry change (Nelsen's π -oxidation line¹³) is presented in Figure 2. Molecules with negligible "relaxation" upon ionization have IP_V and E° values close to the line of Figure 2 ($r = 0.987$, average deviation = 1.2 kcal mol⁻¹). Differential solvation effects can account for small deviations from the line. Azoalkane **1** falls substantially below the "no relaxation" line, and from Figure 2 we estimate the gas-phase relaxation energy for 1^{**} to be roughly 18 kcal mol⁻¹.

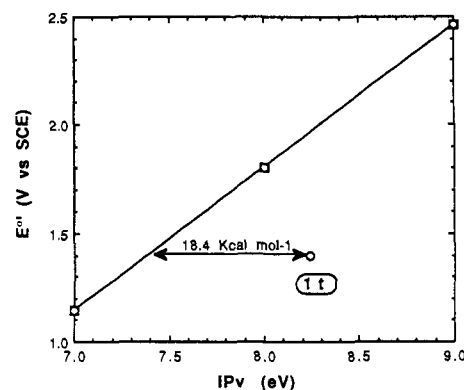


Figure 2. Comparison of $1 E^\circ$ and IP_V values to those of a set¹² of polycyclic arenes, alkylbenzenes, and alkyl peroxides having negligible relaxation energies upon ionization.

Ab initio calculations¹⁴ (6-31G*) of C_{2h} *trans*-azomethane neutral and radical cation structures predict a CNN angle opening of 18° and a N,N bond shortening of 0.069 Å upon electron loss, with $\Delta E_{\text{relax}} = E_{\text{vertical cation}} - E_{\text{optimized cation}} = 21$ kcal mol⁻¹. Both 6-31G*/UHF and AM1/UHF¹⁵ calculations favor a 2A_g ground electronic state (n - radical) for azomethane radical cation in contrast to assignments by Rhodes⁵ of 2A_u ground states (π radicals) for matrix-isolated azoethane (**2**) and azopropane (**3**) radical cations.

The $a_{\text{iso}}(2\text{N}) = 13.0$ G for 1^{**} is much smaller than the 31 G value observed for matrix-isolated 2,3-diazabicyclo[2.2.2]oct-2-ene radical cation⁶ (4^{*+}) (presumably because the latter has constrained small CNN angles) and is considerably larger than the 8 G value estimated for 2^{*+} and 3^{*+} . 1^{**} 's solid-state ESR spectrum is tentatively assigned as $a_z(2\text{N}) = 22$ G, yielding $2B \approx 9$ G.¹⁶ This assignment is consistent with substantial s character in the spin-bearing orbital as predicted for a 2A_g radical cation. Additional work is underway to study 1^{**} in other matrices, examine its deazetation reaction and photochemistry, and investigate the one-electron-oxidation chemistry of **1**'s *cis* isomer. In closing, we note that electron removal from **1** accelerates its thermal deazetation reaction by a factor of roughly 10^{22} at room temperature.^{17,7b}

Acknowledgment. We gratefully acknowledge support from the donors of the Petroleum Research Fund, administered by the

(14) Frisch, M. J.; Binkley, J. S.; Schlegel, H. B.; Raghavachari, K.; Melius, C. F.; Martin, R. L.; Stewart, J. J. P.; Bobowicz, F. W.; Rohlfing, C. M.; Kahn, L. R.; Defrees, D. J.; Seeger, R.; Whiteside, R. A.; Fox, D. J.; Fleuder, E. M.; Pople, J. A. *Gaussian 86*; Carnegie-Mellon Quantum Chemistry Publishing Unit: Pittsburgh PA, 1984.

(15) (a) Dewar, M. J. S.; Zebisch, E. G.; Healy, E. F.; Stewart, J. J. P. *J. Am. Chem. Soc.* **1985**, *107*, 3902. (b) We thank Dr. T. Clark for kindly providing his customized AMPAC program package, SCAMP.

(16) For C_{2h} 1^{*+} , a pure π radical cation (2A_u), having the z direction perpendicular to the CNNC molecular plane, should show $a_z(2\text{N}) \approx 3a_{\text{iso}}(2\text{N})$. This is not the case, and the observed data is better interpreted in terms of a z direction parallel to the CNNC plane of the molecule containing substantial s character as expected for an n - radical cation (2A_g). Broad shoulders on the central features of the dominant a_z component of the spectrum might be interpreted as 8–9-G perpendicular features of the nitrogen hyperfine interaction, but further work is required before a definitive assignment can be made.

(17) We postulate the deazetation rate acceleration to derive in part from a thermodynamic effect. That is, we expect the radical cation deazetation reaction to be more thermodynamically favorable than the neutral deazetation reaction. In fact, such electron transfer mitigated rate acceleration effects may be general for radical-forming reactions from neutral closed-shell reactants because the open-shell products are generally much more easily oxidized than the reactants.¹⁸ In addition, the azoalkane geometric response to one-electron oxidation represents structural progress toward the expected deazetation transition structure so that an azoalkane radical cation may be kinetically "activated" toward deazetation as well.

(18) For some other recent examples of this phenomenon, see: (a) Dinocenzo, J. P.; Conlon, D. A. *J. Am. Chem. Soc.* **1988**, *110*, 2324. (b) Dai, S.; Pappas, R. S.; Chen, G.-F.; Guo, Q.-X.; Wang, J. T.; Williams, F. J. *Am. Chem. Soc.* **1989**, *111*, 8759. (c) Maslak, P.; Narvaez, J. N. *Angew. Chem., Int. Ed. Engl.* **1990**, *29*, 283.

(9) For reviews of the Freon matrix oxidation method, see: (a) Shida, T.; Haselbach, E.; Bally, T. *Acc. Chem. Res.* **1984**, *17*, 180. (b) Shida, T. *Electronic Absorption Spectra of Radical Ions*; Elsevier: New York, 1988. (c) Shiotani, M. *Magn. Reson. Rev.* **1987**, *12*, 333.

(10) The treatment of Th^{*+} with H_2O is known to give equal molar quantities of Th and ThO. Murata, Y.; Shine, H. J. *J. Org. Chem.* **1969**, *34*, 3368.

(11) Engel, P. S.; Gerth, D. B.; Keys, D. E.; Scholz, J. N.; Houk, K. N.; Rozeboom, M. D.; Eaton, T. A.; Glass, R. S.; Broecker, J. L. *Tetrahedron* **1988**, *44*, 6811.

(12) (a) Parker, V. D. *J. Am. Chem. Soc.* **1976**, *98*, 98. (b) Howell, J. O.; Goncalves, J. M.; Amatore, C.; Klasinc, L.; Wightman, R. M.; Kochi, J. K. *J. Am. Chem. Soc.* **1984**, *106*, 3968. (c) Nelsen, S. F.; Teasley, M. F.; Bloodworth, A. J.; Eggelte, H. J. *J. Org. Chem.* **1985**, *50*, 3299.

(13) Nelsen, S. F.; Blackstock, S. C.; Petillo, P. A.; Agmon, I.; Kaftory, M. *J. Am. Chem. Soc.* **1987**, *109*, 5724.

American Chemical Society, and the Vanderbilt University Summer Undergraduate Research Program for a fellowship to M.E.M. We also thank Professor A. H. Beth and David Shroyer for assistance with matrix ESR experiments and Professor S. F. Nelsen for insightful discussions.

Supplementary Material Available: Experimental description of 1^{++} generation for solution ESR and UV-vis studies and Th reduction, description of 1^{++} decomposition with gas-evolution measurement, cyclic voltammogram of **1**, UV-vis spectrum of 1^{++} , and solid-state ESR spectra of 1^{++} in CH_2Cl_2 (6 pages). Ordering information is given on any current masthead page.

Carbonyl Coupling on the $\text{TiO}_2(001)$ Surface

H. Idriss, K. Pierce, and M. A. Barteau*

Center for Catalytic Science and Technology
Department of Chemical Engineering
University of Delaware, Newark, Delaware 19716

Received September 12, 1990

The formation of carbon-carbon bonds is the basis for a number of important catalytic processes, including olefin polymerization, carbonylation, hydroformylation, alkylation, and Fischer-Tropsch synthesis. While surface science studies of reactions on single-crystal surfaces under ultrahigh vacuum conditions have yielded significant information on catalytic oxidation and hydrogenation reactions, there are few examples of carbon-carbon bond formation on surfaces at these pressures. We have previously observed two such reactions which occur on single-crystal surfaces of TiO_2 . Coupling of a pair of adsorbed carboxylates, $\text{C}_n\text{H}_{2n\pm 1}\text{COO}$, to a higher ketone, $(\text{C}_n\text{H}_{2n\pm 1})_2\text{C}=\text{O}$, requires surface Ti(IV) cations with a pair of coordination vacancies.¹⁻³ Aldol condensation of acetaldehyde to crotonaldehyde and crotyl alcohol also takes place on Ti(IV) sites on a fully oxidized surface, but only a single coordination vacancy per surface cation is required.⁴ We report here an additional class of C-C formation reactions involving the carbonyl group: carbonyl metathesis to form higher olefins via



This reaction requires prior partial reduction of the TiO_2 surface.

Carbonyl coupling to olefins can be carried out with a number of metals.⁵ This synthesis with titanium reagents utilizes a slurry of solid TiCl_3 in the presence of a strong reducing agent such as LiAlH_4 , Li, K, or Zn-Cu.⁶ The salient features of this reaction are as follows: (1) The active reagent consists of multiple reduced Ti sites at the solid surface; the oxidation state of these reduced sites is assumed to be Ti(0).^{6,7} (2) The mechanism involves reductive dimerization to form a C-C bond followed by rate-determining, sequential deoxygenation of the 1,2-diolate intermediate.⁶ In contrast, we find no evidence for the presence of Ti(0) on our TiO_2 surfaces under conditions where carbonyl coupling to olefins is appreciable.

The apparatus and the procedures in our studies of TiO_2 single-crystal surfaces have been previously described.^{1,8} X-ray photoelectron spectroscopy (XPS) demonstrated that the disordered, argon ion bombarded (001) surface contained titanium(II), -(III), and -(IV),^{1,8} but there was no evidence for the characteristic $2p_{3/2}$ line of Ti(0) at 454.5 eV, consistent with other reports for sputtered TiO_2 ⁹ and the equilibrium between titanium and its

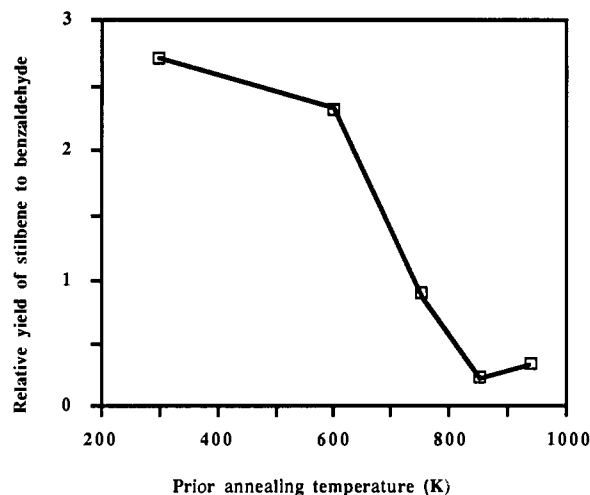
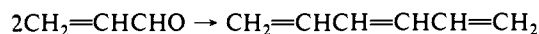
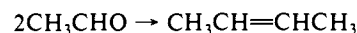


Figure 1. Ratio of stilbene to benzaldehyde desorbed following benzaldehyde adsorption at 300 K on sputtered $\text{TiO}_2(001)$ surfaces previously annealed at 300-930 K.

oxides.¹⁰ Annealing the surface at higher temperatures oxidizes the surface by diffusion from the bulk¹ as evidenced by (1) an increase of the surface O/Ti ratio by Auger electron spectroscopy (AES); (2) attenuation of the Ti(II) and Ti(III) peaks in XPS (these were not detectable after annealing above 750 K); and (3) reconstruction of the surface to a (011)-faceted structure above 750 K.¹¹

We report here the following examples of olefin formation by coupling of aliphatic, α,β -unsaturated, and aromatic aldehydes on the sputtered and low-temperature (below ca. 750-800 K) annealed surfaces:



The ratio of stilbene to benzaldehyde observed in temperature-programmed desorption (TPD) experiments is illustrated in Figure 1. The TiO_2 surface was exposed at 300 K to benzaldehyde from a dosing needle at a background pressure of 1.5×10^{-8} Torr for 100 s. After evacuation, the temperature of the TiO_2 sample was ramped at a rate of 1.2 K/s. Products were detected with an onboard UTI 100C quadrupole mass spectrometer multiplexed with an IBM PC. All masses between 2 and 260 amu were examined in experiments in which 8, 20, 50, or 100 masses were monitored concurrently. Stilbene was identified by the prominent signal for $m/e = 180$ as well as its fragmentation to $m/e = 179, 178, 165, 152, 115,$ and 102 . Quantitative determination of the relative sensitivities¹² from the corresponding fragmentation patterns indicated that the yield of stilbene at 440 K from the sputtered surface was ca. 2.7 times that of the benzaldehyde which desorbed at 385 K.

Annealing the surface at temperatures to 930 K prior to aldehyde adsorption produced a monotonic decrease in the yield of olefins. The stilbene yield from the surface annealed at 850 K was less than 10% of that from a freshly bombarded surface. Since annealing the surface progressively decreases the concentration of Ti(II) and Ti(III) species at the surface to the limits of XPS detection by 750-850 K, the parallel decrease of the stilbene yield from benzaldehyde suggests that the active sites for this reaction are Ti(III) and possibly Ti(II) cations at the surface. The participation of multiple surface cations and the facile rearrangement of lattice oxygen may circumvent the need for a single metallic site, e.g., Ti(0), which can effect a four-electron reduction.

(1) Kim, K. S.; Barteau, M. A. *J. Catal.* **1990**, *125*, 353.

(2) Kim, K. S.; Barteau, M. A. *Langmuir* **1990**, *6*, 1485.

(3) Kim, K. S.; Barteau, M. A.; Idriss, H. *Petroleum Preprints, ACS* **1990**, *35*, 117.

(4) Idriss, H.; Kim, K. S.; Barteau, M. A., manuscript in preparation.

(5) Kahn, B. E.; Rieke, R. D. *Chem. Rev.* **1988**, *88*, 733.

(6) McMurry, J. E. *Chem. Rev.* **1989**, *89*, 1513.

(7) Dams, R.; Malinowski, M.; Westdorp, I.; Geise, H. *J. Org. Chem.* **1982**, *47*, 248.

(8) Kim, K. S.; Barteau, M. A. *Surf. Sci.* **1989**, *223*, 13.

(9) Hoflund, G. B.; Yin, H. L.; Grogan, A. L., Jr. Asbury, D. A.; Yoneyama, H.; Ikeda, O.; Tamura, H. *Langmuir* **1988**, *4*, 346.

(10) Goodenough, J. B. *Prog. Solid State Chem.* **1971**, *5*, 145.

(11) Firment, L. E. *Surf. Sci.* **1982**, *116*, 205.

(12) Ko, E. I.; Benziger, J. B.; Madix, R. J. *J. Catal.* **1980**, *62*, 264.